OXIDATION KINETICS OF NUCLEAR GRADE FeCrAl ALLOYS IN STEAM IN THE TEMPERATURE RANGE 600-1500°C

C. KIM, C. TANG, M. GROSSE, M. STEINBRUECK

Institute for Applied Materials, Karlsruhe Institute of Technology (KIT-IAM)
D-76021 Karlsruhe Germany

C. KIM, C. JANG

Korea Advanced Institute of Science and Technology (KAIST)
34141 Daejeon Republic of Korea

Y. MAENG

Korea Electric Power Corporation-Engineering & Construction company (KEPCO-E&C)
39660 Gimcheon Republic of Korea

ABSTRACT

Thin FeCrAl tubes are promising candidates for ATF cladding application. In this study, the high-temperature oxidation in steam of two nuclear-grade FeCrAl alloys developed by ORNL (B136Y3 and C26M2) was investigated over a wide temperature range. Transient oxidation tests from 500°C to 1250°C were conducted as well as isothermal experiments from 600°C to 1500°C. The well-accepted and in severe accident codes applied low oxidation kinetics determined by the formation of a protective α-alumina scale was confirmed only for the temperature range 1000-1250°C. At lower temperatures, the oxidation kinetics of both alloys followed rather the kinetics of transient alumina such as θ-alumina. At temperatures from approx. 1350°C, protective alumina formation failed resulting in much faster oxidation kinetics determined by the formation of iron oxides. This faster oxidation at low and high temperatures should be taken into account in codes for simulation of accident scenarios. Special effects of small open tube segments allowing oxidation of the inner surfaces and of thin wall thickness are discussed.

1. Introduction

Worldwide efforts have been made to mitigate excessive hydrogen release from the high-temperature cladding oxidation during e.g. nuclear accidents by using alumina-forming alloys [1-3], because alumina-forming alloys show superior oxidation resistance at high temperature and are less expensive than current Zr alloys. Oak Ridge National Laboratory (ORNL) also developed accident tolerant fuel (ATF) claddings based on FeCrAl by reducing the Cr content to mitigate irradiation embrittlement during normal operation [3]. Newly developed nuclear-grade FeCrAl alloys also showed superior oxidation resistance in spite of their low Cr contents [3,4]. They showed a continuous and protective alumina layer at 1200°C. However, data at lower and higher temperatures for the nuclear-grade FeCrAl alloys with a thin thickness are also important to simulate accident scenarios. Only a few literatures reported the oxidation behavior of nuclear-grade FeCrAl alloys below 1000°C and above 1300°C.
Therefore, in this study, nuclear-grade FeCrAl alloys were exposed to the steam atmosphere in a wide temperature range to provide the oxidation kinetics information. Transient oxidation test from 500°C to 1250°C and isothermal oxidation tests from 500°C to 1500°C for 20h were carried out using two nuclear-grade FeCrAl alloys, B136Y3 and C26M2. After the oxidation tests, the

oxides formed on the two nuclear-grade FeCrAl alloys were analysed and the steam oxidation kinetics is discussed.

2. Experimental procedure

Two newly-developed nuclear-grade FeCrAl alloys, B136Y3 and C26M2, were provided by ORNL in a tubular shape. B136Y3 tubes had an outer diameter (OD) of 9.6 mm and a thickness of 0.425 mm, and C26M2 tubes had an OD of 9.6 mm and a thickness of 0.45 mm. The details on the tube manufacturing process can be found elsewhere [5]. To compare the transient oxidation behaviour in steam, two commercial FeCrAl alloys, APM and APMT, were purchased from Sandvik in a rod shape. The chemical compositions for all four FeCrAl alloys are listed in **Table 1**. The chemical compositions of two nuclear-grade FeCrAl alloys were provided by ORNL and chemical compositions of APM and APMT were provided by Sandvik. For oxidation tests, the tubular nuclear-grade FeCrAl alloys were cut to specimens with a length of 10 mm for isothermal oxidation tests at 600°C to 1200°C and 20 mm for the isothermal tests at 1300°C to 1500°C, 15 mm for transient oxidation tests. APM and APMT were also fabricated to disc-type specimens with a thickness of 2 mm and a diameter of 10 mm for APM and 8 mm for APMT. The disc-type specimens were mechanically ground on both sides. The tubular specimens were not additionally ground after the surface treatment at ORNL. All specimens were ultrasonically cleaned in isopropanol prior to the oxidation tests.

wt.%	Fe	Cr	Al	Mo	Y	C	Si	Mn
APM	Bal	20.5-23.5	5.8	-	-	<0.08	<0.7	<0.4
APMT		20.5-23.5	5.0	3.0	-	<0.08	<0.7	<0.4
B136Y3		12.97	6.19	-	0.03	<0.01	-	-
C26M2		11.87	6.22	1.98	0.03	<0.01	0.2	-

Tab 1: Chemical compositions of four FeCrAl alloys used in this study

Two steam oxidation facilities, the STA 449 F3 and a horizontal tube furnace (BOX), were used in this study to evaluate high-temperature oxidation behaviour in steam. The STA 449 F3 is a simultaneous thermal analyser system manufactured by NETZSCH with a water vapour furnace allowing annealing in almost 100% steam atmosphere up to 1250°C. A ceramic ring and Pt meshed sample holders were utilized as sample holder for tubular specimens and ceramic crown structures were used for disc-type specimens to provide access of the oxidizing atmosphere to almost the whole surface. For transient oxidation tests in the STA, Ar gas was supplied via the balance volume with the flow rate of 50 ml/min and the furnace was heated up to 500°C. Then, the furnace was kept for 10 min to stabilize the temperature. After the stabilization, the steam was injected to the test zone with a flow rate of 2 g/h from the top. The furnace temperature increased up to 1250°C with a heating rate of 1 K/min. When the temperature reached 1250°C, the temperature maintained at 1250°C for 10 min. Then, the steam injection was stopped and the furnace was cooled down with a rate of 50K/min.
For isothermal tests, the temperature increased to the target temperature in flowing Ar gas. When the temperature had reached the target, it was kept for 10 min to stabilize the temperature. Then, steam was injected into the test zone and the condition was kept for 20 h. Then, the steam injection and furnace heating were stopped.
Above 1300°C, the so-called BOX facility with higher temperature capability was utilized to evaluate the oxidation behaviour at temperatures. Although the BOX facility is not equipped with an analytical balance, a high-resolution gas mass spectrometer (Balzer GAM300) is placed at

the gas outlet of BOX facility to detect hydrogen release during oxidation tests. A detailed description can be found in a previous study [6]. For the isothermal oxidation tests at above 1300°C, the specimen was loaded on alumina boats with alumina cylinders to hold specimens on the boats and minimalize the contact of specimens and the boats. Ar gas flowed into the test zone with a rate of 20 L/h and the furnace was heated up to the target temperature. The target temperature was kept for 30 min to stabilize the test condition and steam was injected of a flow rate of 20 g/h for 20 h. After the isothermal oxidation tests for 20 h, the heating and steam flow were stopped.

During isothermal oxidation tests in the BOX, hydrogen and Ar release rates were recorded in vol.% and converted into mol/h using Ar as a reference. The hydrogen release rate is proportional to the oxidation rate as following Eq 1. Eq. 2 can be derived from Eq. 1. In Eq. 2, $\Delta m_{oxide}$is weight gain by oxide (M_xO_y) from the oxidation, : Δm_{H_2} weight of H_2 generated by the oxidation, W_{O_2} molecular weight of O_2, W_{H_2} molecular weight of H_2. By using Eq. 2, weight gains as a function of oxidation time and parabolic rate constants of nuclear-grade FeCrAl alloys were calculated for the isothermal oxidation tests above 1300°C.

$$xM + yH_2O \rightarrow M_xO_y + yH_2 \quad (1)$$

$$\Delta m_{oxide} : \Delta m_{H_2} = \frac{1}{2} W_{O_2} : W_{H_2} \approx 8 : 1 \quad (2)$$

To characterize microstructural features of the oxide layers, analytical methods were applied such as optical microscopy (OM, Reichert Jung MeF3) and field-emission scanning electron microscope (SEM, Philips XL30S) equipped with energy-dispersive X-ray spectroscope (EDS).

3. Results and discussion

3.1 Transient oxidation tests from 500°C to 1250°C

Fig 1 shows weight gains of the four FeCrAl alloys during the transient oxidation tests from 500°C to 1250°C. The nuclear-grade FeCrAl alloys with lower Cr content of 12-13 wt.% showed higher weight gain at low temperature between 600°C and 700°C. The slopes of nuclear-grade FeCrAl became flat from 700°C to 800°C for B136Y3 and from 750°C to 900°C for C26M2. Both slopes increased up to 1150°C. After the short second plateau at 1150°C, the slope raised again. On the other hand, the two commercial FeCrAl alloys containing higher Cr content, APM and APMT, exhibited extremely low weight gain up to 800°C and the weight gains increased up to 1000°C. A plateau region was observed from 1000°C to 1150°C and the slopes for commercial FeCrAl alloys raised again. Here, it should be noted that the nuclear-grade FeCrAl alloys showed significant oxidation at low temperature between 600°C and 700°C.

To investigate the oxidation behaviours of two nuclear-grade FeCrAl alloys, cross-sectional oxide morphologies were observed by OM after transient oxidation tests and the results are shown in **Fig 2**. Both nuclear-grade FeCrAl alloys show similar oxidation behaviour. While a thin oxide layer was formed on the outer surfaces, thick oxide layers were formed on the inner surfaces. The thick oxide layers on the inner surface consisted of an outermost thick, porous and bright grey oxide layer and a dense and darker gray oxide layer at the oxide/metal interface. It seems that the amount of the thick oxide layers on the inner surface caused the difference in the weight gain in **Fig 1**. Such thick oxide formation on the inner surface could result from the lower Cr content of nuclear-grade FeCrAl alloys. However, since APM and APMT specimens were disc-shaped and the nuclear-grade FeCrAl specimens were tubular shaped, it is not sure that the thick oxide formation on the inner surface resulted from the lower Cr contents or different specimen geometry. However, it can be said that the thick oxide layers on the inner surface related to the rapid oxidation of nuclear-grade FeCrAl alloys at lower temperature in **Fig 1**. To

confirm the oxidation behaviours of two nuclear-grade FeCrAl alloys at each temperature, isothermal oxidation tests were conducted at 600°C to 1500°C for 20 h.

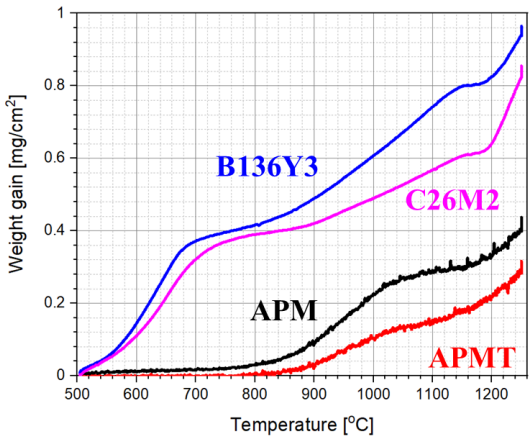

Fig 1. Weight gain of four FeCrAl alloys during transient oxidation test from 500°C to 1250°C

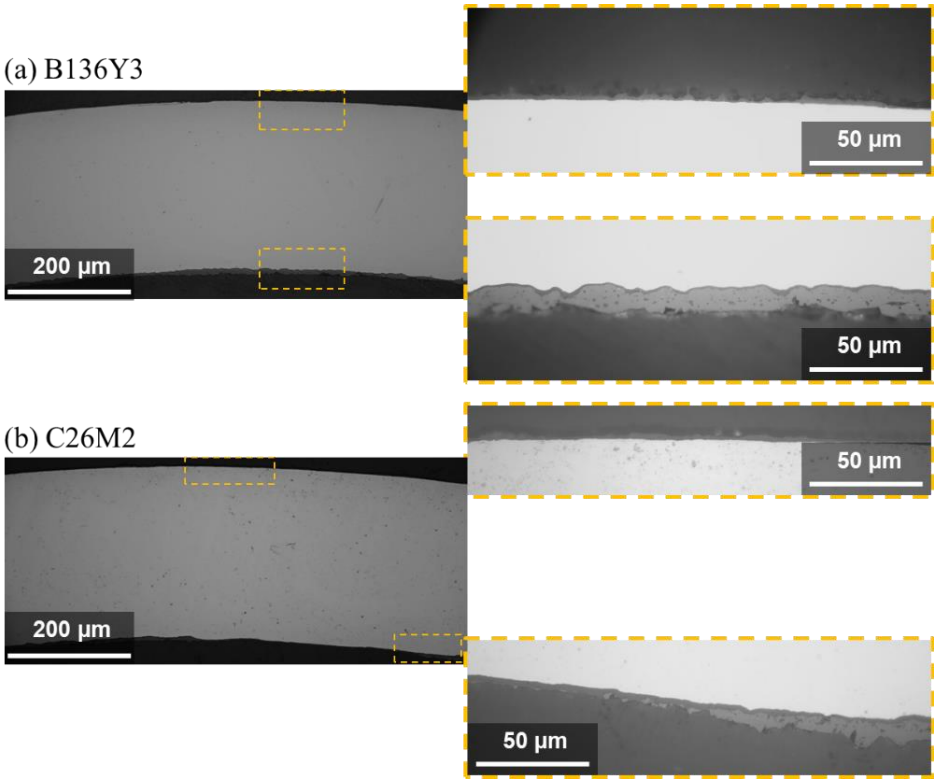

Fig 2. Cross-sectional OM micrographs of (a) B136Y3 and (b) C26M2 after the transient oxidation tests from 500°C to 1250°C

3.2 Isothermal oxidation tests from 500°C to 1500°C

Fig 3 shows weight gains of two nuclear-grade FeCrAl alloys during isothermal oxidation tests at 600°C to 1200°C for 20 h. Both B136Y3 and C26M2 exhibit increased oxidation rates as increasing the test temperatures except of 600°C. The weight gain at 600°C for B136Y3 was similar to the kinetics at 1000°C and C26M2 at 600°C was similar to 1100°C. **Fig 4** shows parabolic rate constants of two nuclear-grade FeCrAl alloys at 600°C to 1500°C with the

parabolic rate constants of θ-alumina [7], α-alumina [8] and Fe-oxide [8] as function of temperature. Both nuclear-grade FeCrAl alloys exhibited faster kinetics than θ-alumina at 600°C and followed the θ-alumina kinetics from 700°C to 800°C. The rate constant at 900°C for B136Y3 and C26M2 is between θ-alumina and α-alumina kinetics. Above 1000°C, the kinetics well followed the α-alumina kinetics up to 1200°C for B136Y3 and 1300°C for C26M2. The kinetics of B136Y3 at 1300°C is between α-alumina and Fe-oxide. When the temperature was higher than 1350°C, both nuclear-grade FeCrAl alloys showed Fe-oxide kinetics, which means that they lost their superior oxidation resistance.

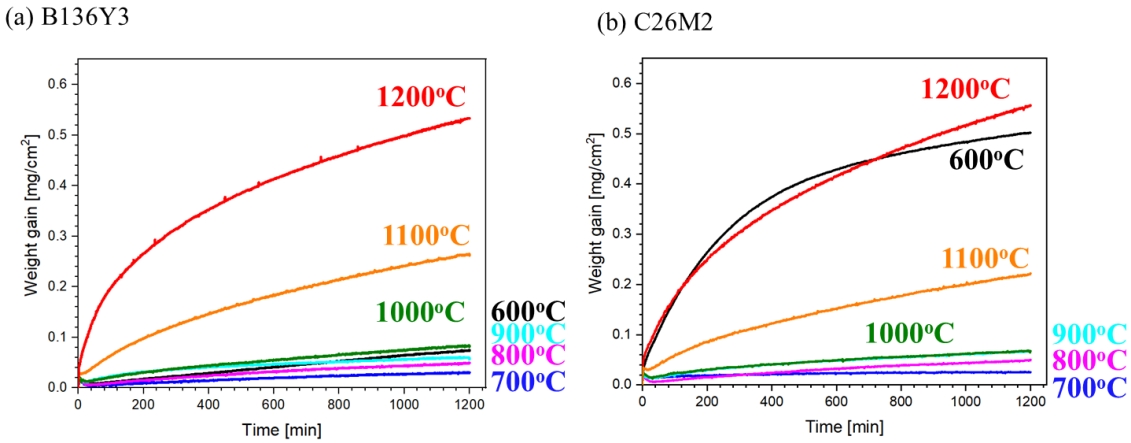

Fig 3. Weight gains of (a) B136Y3 and (b) C26M2 during the isothermal oxidation tests at 600°C to 1200°C

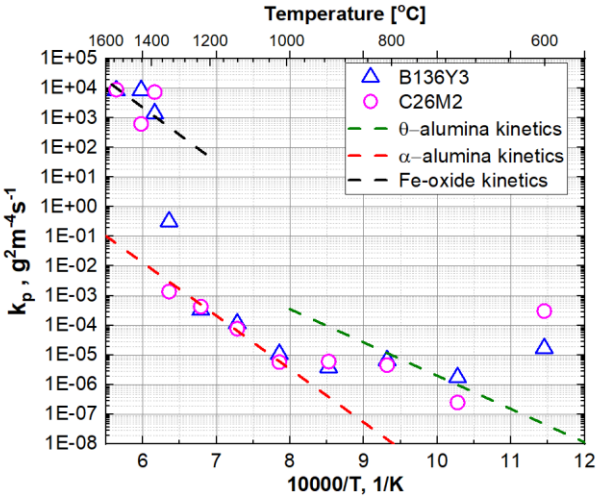

Fig 4. Parabolic rate constants of B136Y3 and C26M2 during the isothermal oxidation tests at 600°C to 1500°C with oxidation kinetics of θ-alumina [7], α-alumina [8] and Fe-oxide [8]

Fig 5 shows macroscopic images of the nuclear-grade FeCrAl alloys before and after steam oxidation tests. Although both bare metal and alumina scale are grey and difficult to distinguish in the current figure, the as-received, 600°C and 700°C look shiny, which means the oxide layer was very thin, and they show metallic appearance. A red-brown inner surface for C26M2 was found at 600°C. From 800°C to 1300°C, there was almost no difference in the macroscopic images. A bright grey oxide layer was formed on the surface, and the original tube shapes were maintained. Above 1350°C, both alloys lost their original tubular shapes. Furthermore, the

kinetics above 1350°C followed Fe-oxide kinetics shown in **Fig 4**. Thus, Fe-oxide would be formed rather than α-alumina above 1350°C. It means that the nuclear-grade FeCrAl tubes lose both their oxidation resistance and their coolable geometry as claddings above 1350°C.

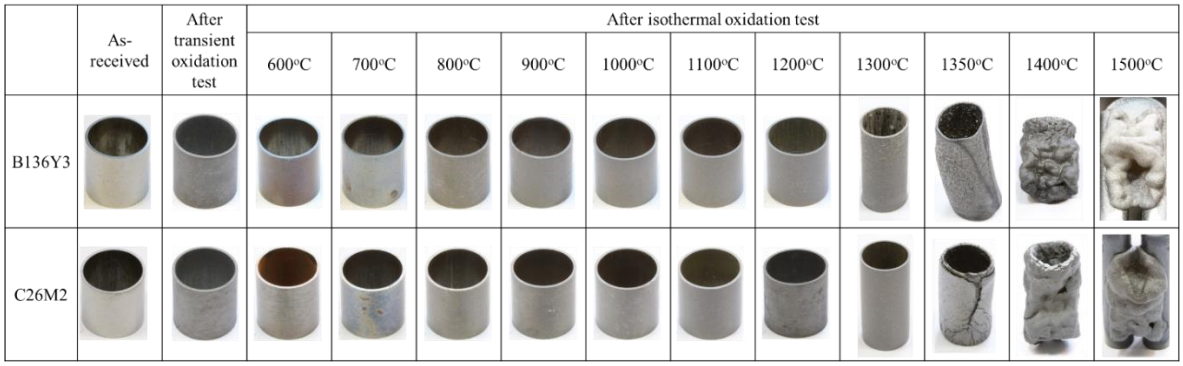

Fig 5. Macroscopic images of B136Y3 and C26M2 after transient oxidation test from 500°C to 1250°C and after the isothermal oxidation tests at 600°C to 1500°C

Fig 6 shows optical micrographs of B136Y3 after isothermal oxidation tests at 600°C to 1300°C. Thick nodular oxides were formed on the inner surface at 600°C. On the other hand, the oxide layer at 600°C on the outer surface was too thin to be observed by OM. The oxide layers at 700°C to 1000°C could not be found due to the thin thickness on both inner and outer surfaces. Thus, the excessive oxidation rate at 600°C resulted from the thick nodular oxides on the inner surface. At 1100°C, the oxide layer on the inner surface (~2 μm) were slightly thicker than on the outer surface (~1.5 μm). Such behaviour was also observed at 1200°C, where the thickness of the oxide layer on the inner surface was ~4 μm and the oxide thickness on outer surface was ~3 μm. As compared with the weight gain in **Fig 3a**, both weight gain and oxide thickness at 1200°C were also twice higher than at 1100°C. At 1300°C, the oxide layer looked convoluted with a thickness of ~6.5 μm on both inner and outer surfaces.

Fig 7 shows optical micrographs of C26M2 after isothermal oxidation tests at 600°C to 1300°C. While B136Y3 exhibited thick nodular oxides on the inner surface at 600°C, C26M2 showed thick oxide layers (~15μm) on the inner surface. On the other hand, the oxide layer is very thin on the outer surface hardly observed by OM like B136Y3 at 600°C. Similar to B136Y3, oxide layers from 700°C to 1000°C were also too thin to be detected and measured by OM on both inner and outer surfaces of C26M2. Thus, due to the thick oxide layer on the inner surface at 600°C, C26M2 at 600°C showed much higher weight gain than 1000°C in **Fig 3b**. At 1100°C, alumina layers of ~ 2 μm were found on the inner and outer surfaces. In addition, the thickness of the alumina layer on the outer surface increased to ~3 μm at 1200°C and ~6 μm at 1300°C, and the oxide thickness on the inner surface increased to ~4 μm at 1200°C and ~7 μm at 1300°C. C26M2 also exhibited different oxide thickness on the inner and outer surface at 1200°C and 1300°C, although the very small difference was observed at 1100°C due to low magnification of OM.

As can be seen in **Fig 6h** and **Fig 7h,** oxidation behaviours of both alloys at 1300°C showed different oxide morphology. While B136Y3 showed the convoluted oxide layer at 1300°C, C26M2 showed a planar oxide layer at 1300°C. Such behaviour would be caused by the higher kinetics of B136Y3 at 1300°C in **Fig 4**. The convoluted oxide morphology is prone to spallation. It can cause more rapid consumption of Al by further oxidation. When the Al content is below the critical Al content to produce a continuous alumina layer, Fe-rich oxide can be formed at high temperature with intermediate Cr content [9]. Therefore, Fe-rich oxides were formed on some parts of B136Y3 at 1300°C, and it showed intermediate kinetics in between Fe-oxide and

alumina in **Fig 4**. However, it needs more oxide analyses to support the Fe-rich oxide formation on B136Y3 at 1300°C.

The oxidation kinetics and oxide morphologies matched well with the kinetics and oxides in literature above 700°C. However, the thick nodular oxides and oxide layers on the inner surface of both alloys at 600°C could not be estimated due to limited studies. To characterize the oxides formed on two nuclear-grade FeCrAl alloys at 600°C, SEM-EDS analyses were conducted, the results are shown in **Fig 8** and **Fig 9**. While a thin Al-rich oxide layer was formed on the outer surface of B136Y3, the nodular oxides consisted of two layers of outermost Fe-rich oxides and underlying Fe,Cr,Al-rich oxides. In addition, the oxide layer next to the nodular oxides was enriched in Cr. **Fig 9** also shows a thin Al-rich oxide layer on the outer surface and two thick layers on the inner surface of C26M2. Since Fe- and Cr-rich oxides have much faster oxidation kinetics than alumina [7,8], the amount of Fe- and Cr-rich oxides formed on the inner surface caused much faster oxidation kinetics at 600°C in **Fig 4**.

Fig 6. Optical micrographs of B136Y3 after the isothermal oxidation tests at (a) 600°C to (h) 1300°C

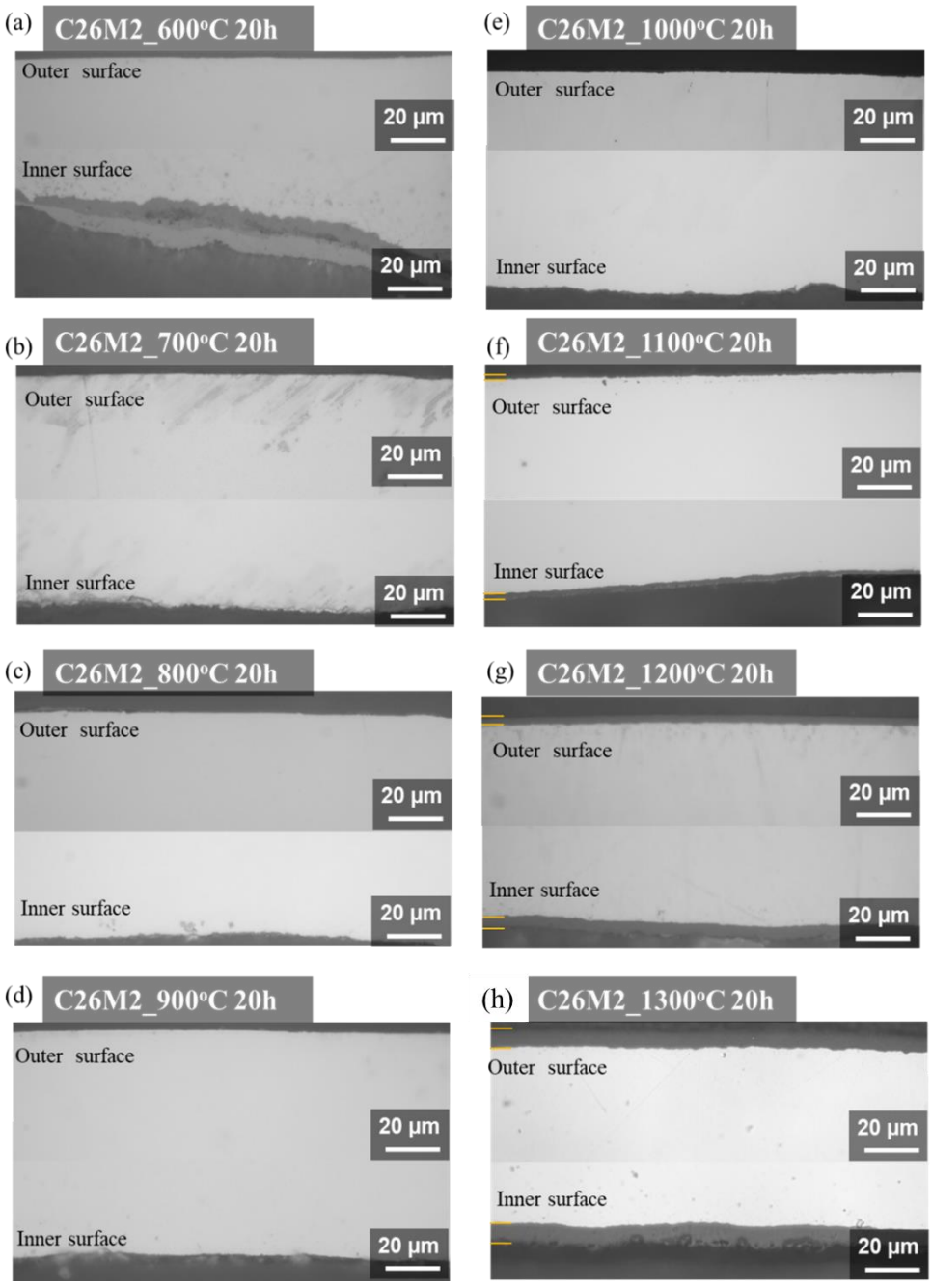

Fig 7. Optical micrographs of C26M2 after the isothermal oxidation tests at (a) 600°C to (h) 1300°C

As shown in the micrographs by OM and SEM, different oxides at 600°C and alumina thickness were found on the inner surface and the outer surfaces of tubes. This was also found in literature using a similar nuclear-grade FeCrAl model alloy with 13Cr-5Al-2Mo in wt.% at 1190°C in air and 1500°C in steam [10]. The FeCrAl alloy in the literature showed alumina on the outer surface, but thick Fe-rich oxide layers on the inner surface at 1190°C in air. Such behaviour could result from the different surface finish for the inner and outer surfaces. However, more analyses are needed to support the assumption. Moreover, the failure of protective oxide layers

and excessive oxidation above 1350°C should be analysed. Finally, it should be mentioned that some of the effects observed in this study might be caused by the small and open sample geometry causing edge effects and oxidation of the inner surfaces, which would not be relevant for application as ATF cladding tubes.

4. Summary

The steam oxidation behaviour of two nuclear-grade FeCrAl tubes (B136Y3 and C26M2) was investigated in a wide temperature range. Transient oxidation tests from 500°C to 1250°C and isothermal tests at 600°C to 1500°C for 20 h were performed. Through the weight gain, hydrogen release rate, and microstructural analyses, it was found that the steam oxidation behaviour of both alloys could be divided in three temperature ranges. Below 900°C, the oxidation kinetics of both alloys followed the kinetics of transient alumina such as θ-alumina. From 1000°C to 1250°C, kinetics determined by the formation of protective α-alumina is observed for the nuclear-grade FeCrAl alloys resulting in a thin and continuous oxide layer. Above 1350°C, the protective alumina failed and the kinetics followed much faster Fe-oxide kinetics. In addition, rapid oxidation kinetics at 600°C was observed for both B136Y3 and C26M2 by showing the thick Fe- and Fe,Cr,Al-rich oxides on the inner surfaces. Further works are needed to characterize the oxides at each temperature and fully understand the different oxidation behaviours of the inner and outer surfaces and Fe-oxide formation above 1350°C.

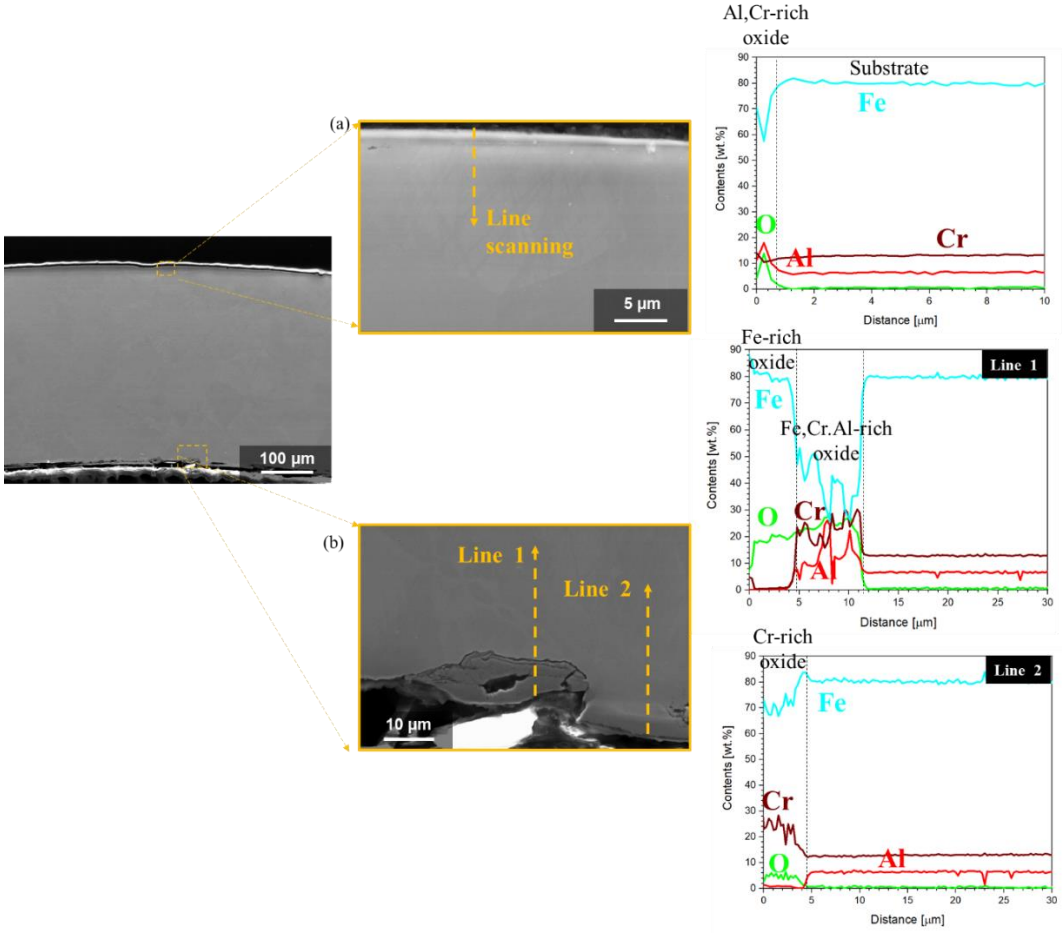

Fig 8. Cross-sectional SEM images and EDS line scanning results for (a) outer surface and (b) inner surface of a B136Y3 tube after isothermal oxidation test at 600°C

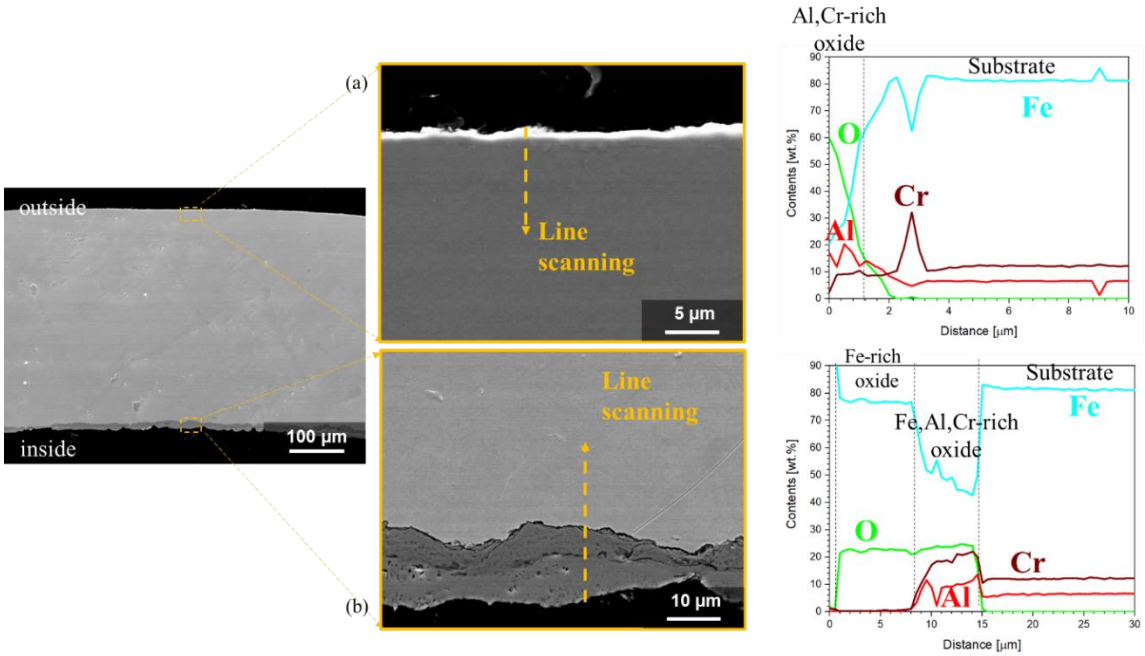

Fig 9. Cross-sectional SEM images and EDS line scanning results for (a) outer surface and (b) inner surface of a C26M2 tube after isothermal oxidation test at 600°C

5. Reference

[1] Z. Duan, H. Yang, Y. Statoh, K. Murakami, S. Kano, Z. Zhao, J. Shen, H. Abe, Current status of materials development of nuclear fuel cladding tubes for light water reactors, Nucl. Eng. Des. 316 (2017) 131-150

[2] H. Kim, H. Jang, G.O. Subramanian, C. Kim, C. Jang, Development of alumina-forming duplex stainless steels as accident-tolerant fuel cladding materials for light water reactors, J. Nucl. Mater. 507 (2018) 1-14

[3] Y. Yamamoto, B.A. Pint, K.A. Terrani, K.G. Field, Y. Yang, L.L. Snead, Development and property evaluation of nuclear grade wrought FeCrAl fuel cladding for light water reactors, J. Nucl. Mater. 467(2) (2015) 703-716

[4]] K.A. Unocic, Y. Yamamoto, B.A. Pint, Effect of Al and Cr content on air and steam oxidation of FeCrAl alloys and commercial APMT alloy, Oxid. Met. 87 (2017) 431-441

[5] Z. Sun, Y. Yamamoto, Processability evaluation of a Mo-containing FeCrAl alloy for seamless thin-wall tube fabrication, Mater. Sci. Eng. A 700 (2017) 554-561

[6] C. Tang, A. Jianu, M. Steinbrueck, M. Grosse, A. Weisenburger, H.J. Seifert, Influence of composition and heating schedules on compatibility of FeCrAl alloys with high-temperature steam, J. Nucl. Mater. 511 (2018) 496-507

[7] G.C. Rybicki, J.L. Smialek, Effect of the θ-α-Al2O3 transformation on the oxidation behavior of β-NiAl + Zr, Oxid. Met. 31(3/4) (1989) 275-304

[8] B.A. Pint, K.A. Terrani, Y. Yamamoto, L.L. Snead, Material selection for accident tolerant fuel cladding, Metall. Mater. Trans. E 2 (2015) 190-196

[9] I. Kvernes, M. Oliveria, P. Kofstad, High temperature oxidation of Fe-13Cr-xAl alloys in air/H2O vapour mixtures, Corros. Sci. 17 (1977) 237-252

[10] B.A. Pint, Performance of FeCrAl for accident-tolerant fuel cladding in high-temperature steam, Corros. Rev. 35(3) (2017) 167-175